

Argand-diagram representation of transition amplitudes for resonant reactive scattering: $e + \text{HCl}$ and $e + \text{H}_2$

C. K. Lutrus and S. H. Suck Salk

*Department of Physics and Graduate Center for Cloud Physics Research, University of Missouri-Rolla,
Rolla, Missouri 65401*

(Received 15 July 1988)

Resonances for rearrangement collisions (reactive scattering) involving the two dissociative attachment processes, $e + \text{HCl} \rightarrow \text{H} + \text{Cl}^-$ and $e + \text{H}_2 \rightarrow \text{H} + \text{H}^-$, are examined. It is shown from the Argand-diagram representation of transition amplitudes that strong resonance is present in the former but not in the latter. That is, the strong resonance is evidenced by the clear exhibition of a phase change by π in a counterclockwise direction in the Argand diagram as the collision energy increases. Such a manifest phase change is absent in the dissociative attachment process of $e + \text{H}_2 \rightarrow \text{H} + \text{H}^-$. This is attributed to the presence of equally strong, direct, and resonant scattering processes, and to the strong influence of mutually destructive interference.

I. INTRODUCTION

Resonant scattering involving electron-molecule systems is well known. Recently, resonant processes associated with rearrangement collisions (reactive scattering) involving the dissociative attachment processes of $e + AB \rightarrow A + B^-$ have been much examined.¹⁻¹² However, explicit studies on competition between direct and resonant processes in reactive scattering have often been neglected. It is of great interest to study such competition and to find differences in the strength of the resonance that appears in various dissociative attachment processes. In the present study, we explore the two different systems of $e + \text{H}_2$ and $e + \text{HCl}$ with regard to the contribution of resonance to the dissociative attachment processes.

Recently, we¹ derived an expression for the transition amplitude equivalent to the theory of Domcke and co-workers² for studying resonance phenomena in reactive scattering involving electron-molecule systems. By closely following their calculational procedure, we were able to reproduce their cross sections for both $e + \text{H}_2 \rightarrow \text{H} + \text{H}^-$ and $e + \text{HCl} \rightarrow \text{H} + \text{Cl}^-$. Despite its merit, the Argand diagram¹³ has seldom been introduced for the study of resonance, particularly in association with rearrangement collisions (reactive scattering). Recently, Kuppermann¹⁴ reported an extensive study of resonance using the Argand diagram for reactive scattering involving atom-diatomic-molecule systems. In this paper, we introduce the Argand-diagram representation of the transition amplitude for dissociative attachment processes associated with electron-molecule systems.

II. RESONANT REACTIVE SCATTERING OF $e + \text{H}_2$ AND $e + \text{HCl}$

Based on our earlier T -matrix study¹ which led to the same expression as that of Mundel, Berman, and Domcke,^{2(a)} we write the transition amplitude of dissociative attachment $e + AB \rightarrow A + B^-$ as

$$T = \langle \chi_d^{0(-)} | (1 + \tau G_1^{(+)}) \tilde{V}_{dc}^\dagger | \tilde{\phi}_c^0 \rangle, \quad (2.1a)$$

or

$$T = \langle \chi_d^{0(-)} | \tilde{V}_{dc}^\dagger | \tilde{\phi}_c^0 \rangle + \langle \chi_d^{0(-)} | \tau G_1^{(+)} \tilde{V}_{dc}^\dagger | \tilde{\phi}_c^0 \rangle. \quad (2.1b)$$

Here $\langle \chi_d^{(-)} |$ is the scattering state in the final arrangement of $A + B^-$; \tilde{V}_{dc}^\dagger , the coupling potential matrix¹ between electronic continuum and discrete states; and $|\tilde{\phi}_c^0\rangle$, the unperturbed molecular vibrational state of molecule AB . τ is defined as

$$\tau = F(F - FG_1^{(+)}F)^{-1}F, \quad (2.2)$$

where

$$F = \Delta - i\Gamma/2, \quad (2.3)$$

Δ and Γ are the energy shift and energy width, respectively, and $G_1^{(+)}$ is the Green's function^{1,2} describing the propagation of the H_2^- (or HCl^-) state. The first term in (2.1b) above is the direct process. The second term represents the indirect process (resonant scattering) due to coupling between the electronic continuum and discrete states. Information on the energy shift and energy width is embedded in the expression of τ .^{1,2}

Following closely the calculational procedure in Ref. 2 we have reproduced the cross sections of $e + \text{H}_2(v) \rightarrow \text{H} + \text{H}^-$ and $e + \text{HCl}(v) \rightarrow \text{H} + \text{Cl}^-$. Here v is the vibrational quantum number of the molecule H_2 or HCl . Part of the calculational procedures involves the use of recursion relations² for the evaluation of the Green's function by introducing the Lanczos basis.¹⁵ In the present calculations, we evaluate the overlap between the scattering state $\langle \chi_d^{0(-)} |$ and the Lanczos basis state differently from Ref. 2. We use a newly discovered recursion method¹⁶ which was found to be simple to use and of great accuracy. For the sake of self-containment, we reintroduce the computed result¹ of each term in (2.1b) above, in order to examine separately the contributions of the direct scattering (first term) and resonant scattering (second term) processes to the total cross section. Figures 1(a)–1(c) show the cross sections of the dissociative

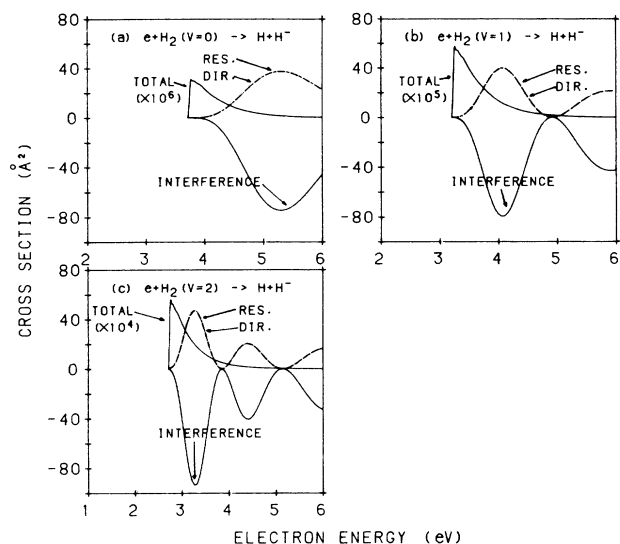


FIG. 1. Total (TOTAL), resonant (RES.), and direct (DIR.) cross sections, including the contribution of interference effect for the dissociative attachment process, $e + \text{H}_2(v) \rightarrow \text{H} + \text{H}^-$ as a function of electron collision energy for (a) $v=0$, (b) $v=1$, and (c) $v=2$. The total cross sections for $v=0, 1$, and 2 are magnified by the factors of $10^6, 10^5$, and 10^4 , respectively. The resonant cross sections are seen to coincide with the direct cross sections.

attachment process $e + \text{H}_2(v) \rightarrow \text{H} + \text{H}^-$ involving the low-lying vibrational states of $v=0, 1$, and 2 of H_2 . The total cross sections (denoted TOTAL in the figures) represent the sum of the direct (denoted DIR.) and resonant (denoted RES.) processes, and their interference effect. It is to be noted that the total cross sections for the vibrational states $v=0, 1$, and 2 are magnified by the factors of $10^6, 10^5$, and 10^4 , respectively. Both the direct and resonant processes yielded the maximum values of their cross sections nearly at the same electron collision energies for all the cases of initial vibrational states. Further, we note nearly indistinguishable structures between the two processes. We find that interference between the two processes is destructive in this region of collision energies. This implies that the phase of transition amplitude between the two is opposite (i.e., $\sim 180^\circ$ apart). The same phase difference of $\sim 180^\circ$ is also found to occur near and at the collision energies where the peaks of the total cross sections appear, as shown in Figs. 2(a)–2(c). It is of note that the total cross sections in Figs. 2(a)–2(c) are magnified by a factor of 1000. Figures 3(a)–3(c) exhibit the total, direct, and resonant cross sections, and their interference effects for $e + \text{HCl}(v) \rightarrow \text{H} + \text{Cl}^-$ with $v=0, 1$, and 2 . Except for the collision energy region where the peak of the total cross section occurs, we observe nearly indistinguishable structures for the direct and resonant cross sections and the phase difference of $\sim 180^\circ$ between the direct and resonant part of transition amplitude. This feature is the same as was seen in $e + \text{H}_2 \rightarrow \text{H} + \text{H}^-$. Sharp distinction in the contribution of resonance to the dissociative attachment processes is found only in the region of collision energy

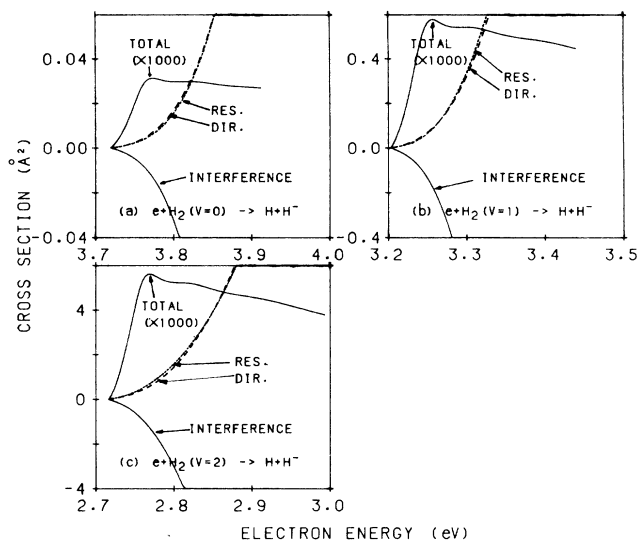


FIG. 2. Enlargement of Fig. 1 for the peak regions of the total cross sections. The total cross sections are magnified by a factor of 1000.

where the peak of the total cross section appears.

In order to reveal a sharp distinction in the contribution of resonance to the dissociative attachment processes, we now introduce the Argand-diagram representation of the transition amplitude for both $e + \text{H}_2 \rightarrow \text{H} + \text{H}^-$ and $e + \text{HCl} \rightarrow \text{H} + \text{Cl}^-$. If resonance is prevalent, the value of the transition amplitude moves about a semicircle in a counterclockwise direction as the collision energy increases.^{14,17,18} That is, the resonant part of phase quickly

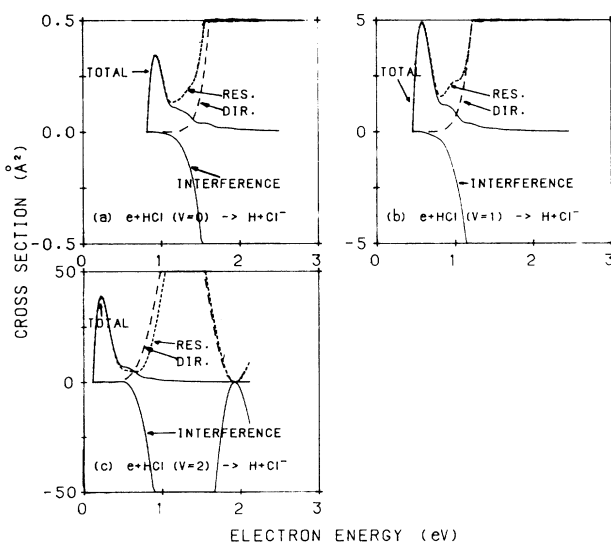


FIG. 3. Total (TOTAL), resonant (RES.), and direct (DIR.) cross sections including the contribution of interference effect for the dissociative attachment process, $e + \text{HCl}(v) \rightarrow \text{H} + \text{Cl}^-$ as a function of electron collision energy for (a) $v=0$, (b) $v=1$, and (c) $v=2$. The total cross sections are seen to coincide with the resonant cross sections near and at the peak position.

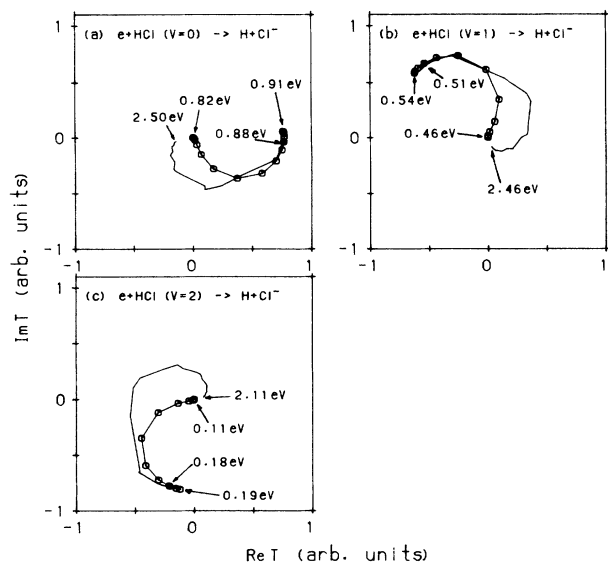


FIG. 4. Argand diagram of transition amplitude for $e + \text{HCl} \rightarrow \text{H} + \text{Cl}^-$. The solid circles denote the electron collision energies E_k where the peaks of the total cross sections occur. For (a) $v=0$, the open circles are placed at an interval of 0.006 eV from $E_k = 0.82$ eV to 0.91 eV and the peak position is located at $E_k = 0.88$ eV; for (b) $v=1$, the open circles are placed at an interval of 0.007 eV from $E_k = 0.46$ eV to 0.54 eV, and the peak position is located at $E_k = 0.51$ eV; for (c) $v=2$, the open circles are placed at an interval of 0.007 eV from $E_k = 0.11$ eV to 0.19 eV and the peak position is located at $E_k = 0.18$ eV. The Argand diagram is plotted in an arbitrarily normalized scale.

increases by π while the direct (background) part of the phase remains nearly unchanged, as the energy increases. Figures 4(a)–4(c) are the Argand diagrams for the transition amplitude of $e + \text{HCl} \rightarrow \text{H} + \text{Cl}^-$. In all cases semicircles in a counterclockwise direction are noticeably exhibited as the energy increases. For $v=0$, the open circles are placed at an interval of 0.006 eV. The semicircle starts at the collision energy of $E_k = 0.82$ eV and ends at $E_k = 0.91$ eV. The peak of the total cross section (denoted by solid circles) is found to occur at $E_k = 0.88$ eV. For $v=1$ and 2 , the open circles are placed at an interval of 0.007 eV. For $v=1$, the semicircle starts from 0.46 eV and ends at 0.54 eV. For $v=2$, it starts from 0.11 eV and ends at 0.19 eV. The peak positions of the total cross sections for $v=1$ and 2 are found to occur at 0.51 eV and 0.18 eV, respectively. Beyond the counterclockwise semicircles, the values of the transition amplitudes are seen to turn clockwise, as the collision energy further increases.

As shown in Figs. 1 and 2, there exists no dominant term that contributes to the total cross section for $e + \text{H}_2 \rightarrow \text{H} + \text{H}^-$, unlike the case of $e + \text{HCl} \rightarrow \text{H} + \text{Cl}^-$. Interestingly, both the direct and resonant terms are observed to be nearly equal in strength, but they are in opposite phase with the phase difference of $\sim 180^\circ$. This

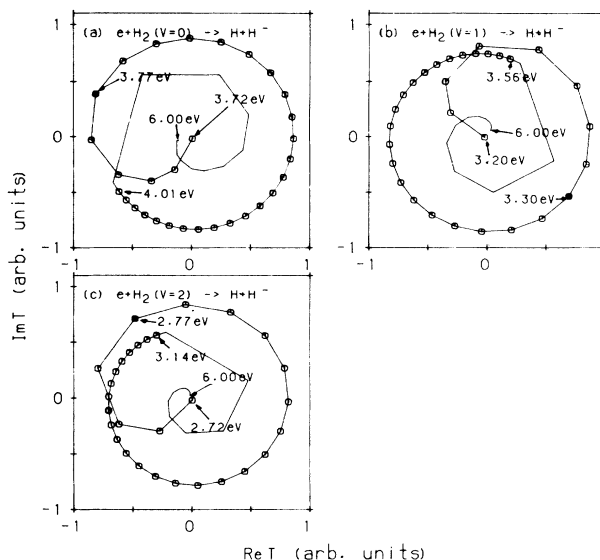


FIG. 5. Argand diagram of transition amplitude for $e + \text{H}_2 \rightarrow \text{H} + \text{H}^-$. The solid circles denote the electron collision energies E_k where the peaks of the total cross sections occur. The open circles are placed at an interval of 0.01 eV. For (a) $v=0$, the peak position is located at $E_k = 3.77$ eV; for (b) $v=1$, the peak position is located at $E_k = 3.30$ eV; and for (c) $v=2$, the peak position is located at $E_k = 2.77$ eV. The Argand diagram is plotted in an arbitrarily normalized scale.

will result in the large contribution of destructive interference to lessen the effect of resonance. Thus counterclockwise rotation in the complex plane of transition amplitude is not likely to occur. Indeed, such rotation in the transition amplitude for $e + \text{H}_2 \rightarrow \text{H} + \text{H}^-$ is absent as shown in Figs. 5(a)–5(c). The open circles are placed at an interval of 0.01 eV. For $v=0, 1$, and 2 , the peak positions of the total cross sections are found to occur at $E_k = 3.77$ eV, 3.30 eV, and 2.77 eV, respectively. In all cases, clockwise rotation in the phase angle is observed as the energy increases. This manifests that the reactive scattering system of $e + \text{H}_2$ is markedly different from $e + \text{HCl}$ in the contribution of resonance to the dissociation attachment process.

III. SUMMARY

In the present paper, the Argand-diagram representation of the T matrix was discussed to sharpen differences in resonance phenomena among various dissociative attachment processes. We have found that in $e + \text{HCl} \rightarrow \text{H} + \text{Cl}^-$ the resonant scattering completely dominates over the direct scattering, unlike the case of $e + \text{H}_2 \rightarrow \text{H} + \text{H}^-$. In $e + \text{H}_2 \rightarrow \text{H} + \text{H}^-$, we have noted comparable competition between the direct and resonant processes and the significance of their destructive interference. Such a marked distinction was well manifested from the Argand diagrams that we investigated here.

- ¹S. H. Suck Salk and C. K. Lutrus, *Phys. Rev. A* **38**, 3388 (1988).
- ²(a) C. Mundel, M. Berman, and W. Domcke, *Phys. Rev. A* **32**, 181 (1985); (b) W. Domcke and C. Mundel, *J. Phys. B* **18**, 4491 (1985).
- ³J. C. Y. Chen, *Phys. Rev.* **148**, 66 (1966); **156**, 12 (1967).
- ⁴T. F. O'Malley, *Phys. Rev.* **150**, 14 (1966).
- ⁵J. N. Bardsley, *J. Phys. B* **1**, 349 (1968); **1**, 365 (1968); J. M. Wadehra and J. N. Bardsley, *Phys. Rev. Lett.* **41**, 1795 (1978); J. N. Bardsley and J. M. Wadehra, *Phys. Rev. A* **20**, 1398 (1979); J. M. Wadehra, *ibid.* **29**, 106 (1984).
- ⁶R. Abouf and D. Teillet-Billy, *J. Phys. B* **10**, 2261 (1977).
- ⁷A. U. Hazi, A. E. Orel, and T. N. Rescigno, *Phys. Rev. Lett.* **46**, 918 (1981).
- ⁸D. Teillet-Billy and J. P. Gauyacq, *J. Phys. B* **17**, 4041 (1984).
- ⁹C. F. Wong and J. C. Light, *Phys. Rev. A* **33**, 954 (1985).
- ¹⁰H. D. Meyer, *Phys. Rev. A* **34**, 1797 (1986).
- ¹¹A. P. Hickman, *J. Phys. B* **20**, 2091 (1987).
- ¹²K. Nakashima, H. Takagi, and H. Nakamura, *J. Chem. Phys.* **86**, 726 (1987).
- ¹³The Argand diagram is a representation of complex numbers. See E. T. Whittaker and G. N. Watson, *Modern Analysis* (Cambridge University Press, New York, 1958), p. 9.
- ¹⁴A. Kuppermann, *Reactive Scattering Resonances and Their Physical Interpretation: The Vibrational Structure of the Transition State*, in *Potential Energy Surface and Dynamics Calculations*, edited by D. G. Truhlar (Plenum, New York, 1981), p. 375; G. C. Schatz and A. Kuppermann, *J. Chem. Phys.* **59**, 964 (1973).
- ¹⁵C. Lanczos, *J. Res. Natl. Bur. Stand.* **45**, 367 (1950); E. W. Knapp and D. J. Diestler, *J. Chem. Phys.* **67**, 4969 (1977).
- ¹⁶C. K. Lutrus and S. H. Suck Salk, *Phys. Rev. A* **37**, 3151 (1988).
- ¹⁷E. Merzbacher, *Quantum Mechanics* (Wiley, New York, 1970), p. 240.
- ¹⁸J. R. Taylor, *Scattering Theory* (Krieger, Malabar, FL, 1983), pp. 240 and 241.